Available online at www.sciencedirect.com
ScienceDirect
Ceramics International 35 (2009) 2781–2787
CERAMICS INTERNATIONAL
www.elsevier.com/locate/ceramint

Phase content and dielectrical properties of sintered BaSrTiO ceramics prepared by a high temperature hydrothermal technique

K.A. Razak [b], A. Asadov [a,*], W. Gao [a]

[a] Department of Chemical and Materials Engineering, The University of Auckland, Private Bag 92019, Auckland, New Zealand
[b] School of Material and Mineral Resources Engineering, University Sains Malaysia, 14300 Nibong Tebal, Penang, Malaysia

Received 16 June 2008; received in revised form 3 February 2009; accepted 14 March 2009
Available online 15 April 2009

Abstract

$Ba_xSr_{1-x}TiO_3$ ceramic powders with varying barium content were prepared by a high temperature hydrothermal technique and sintered at 1300 °C for 1–8 h. Their dielectrical, phase and structural properties were investigated. It was computed from the XRD spectra that the samples with a small amount of strontium, no more than 10% of the initial Ba:Sr share, had a single phase structure with $x = 0.77–0.79$ and Curie point $T_c = 37–53$ °C. Samples with a higher initial Sr ratio developed a two-phase structure and two Curie points. $T_c(x)$ dependence showed that all the experimental data followed a linear trend and were close to the values obtained from the conventional solid state technique, while the dielectric constant was almost one order of magnitude smaller.

Keywords: A. Powders: chemical preparation; B. X-ray methods; C. Dielectric properties; D. $BaTiO_3$ and titanates

1. Introduction

Barium strontium titanate, $Ba_xSr_{1-x}TiO_3$ (BST), is a dielectric material with ferroelectric properties which are tailorable by changing the ratio of barium and strontium. It was first developed and studied in 1940s [1–3] as a way of decreasing (tune) the Curie temperature of BT ceramics from 120 °C down to room temperature for application in electronic devices. Its high dielectric constant, low dielectric loss and high polarisation is used in capacitor and DRAM applications [4,5]. Its high tunability makes it suitable for applications in phase shifters and microwave devices [6–9].

BST powders produced by a conventional solid state technique [1–3,10] have a large grain size and are easily contaminated due to repeated grinding and heat treatment. In our previous work [11–13] we have successfully produced BST powder with a well developed crystalline structure, fine (nano)particle size and a narrow size distribution using a high temperature hydrothermal technique at 220 °C. However, it was found to be difficult to control the stoichiometry of the final products due to the preferential incorporation of Sr than Ba into the structure [14,15]. The phase content of the samples was thoroughly investigated and it was shown that if the molar ratio of the initial compounds was set for a stoichiometric $Ba_xSr_{1-x}TiO_3$ compound, then the final product had a multi-phase structure with significant Ba losses. For a small initial value of Sr = 10–25% it consisted of a two-phase structure, while for a higher concentration of Sr it contained a triple-phase structure.

As BST powder prepared by the hydrothermal technique is a raw material which has to be pressed and sintered for use in possible electronic applications further changes of the material's properties may take place. The aim of this research was to define the phase content changes of the BST after sintering, determine the correlation between the phase content and the dielectrical properties and investigate influence of sintering time on the parameters of the samples.

2. Sample preparation

BST powders with initial Ba/(Ba + Sr) mol ratios of 0.75, 0.80, 0.85 and 0.90 were prepared using a high temperature hydrothermal technique as reported before [11]. Starting materials $BaCl_2{\cdot}2H_2O$ and $SrCl_2{\cdot}6H_2O$ were added into distilled

* Corresponding author. Tel.: +64 9 3737599x87258; fax: +64 9 3737463.
E-mail address: a.asadov@auckland.ac.nz (A. Asadov).

0272-8842/$36.00
doi:10.1016/j.ceramint.2009.03.020

water containing 1.2 M of NaOH and continuously stirred at 80 °C for 2 h. The solution was then filtered and mixed with 0.25 M TiO_2 powder (100% anatase) in an autoclave. The autoclave was placed in a pre-heated oven for 16 h at 220 °C for hydrothermal reaction. The resulting obtained powder was filtered, washed three times using water of pH 12 adjusted by NH_4OH, filtered again and dried. At this stage, as it was reported before [11], the samples were mixtures of two $Ba_xSr_{1-x}TiO_3$ compounds with different x values.

Finally, the powders were mixed with 2% polyvinyl alcohol (PVA) and pressed at 250 MPa to form discs with 11 mm diameter. The discs were further cold isostatically pressed to improve their density, heat treated at 500 °C to remove PVA and then sintered at 1300 °C for 1, 3, 5 and 8 h. Before the experiments all of the samples were polished to remove of about 0.2 mm of the surface layer, as it was found to have different properties from the bulk of the material.

3. Experimental technique

The crystal structure of the uncrushed samples, prepared as described above, was studied using a D8 Advance Bruker X-ray Diffractometer fitted with a Gobbel mirror using Cu Kα radiation. The spectra obtained were analysed with a peak fit software Fityk 0.0.4 (www.fityk.sf.net) in order to separate contributions of $Ba_xSr_{1-x}TiO_3$ compounds with different cell parameters a and c (see also [11]). The parameter x was then determined from the Vegard's law $a(x)$) using data from 79-2265, 34-0411, 44-0093, 39-1395 and 79-0175 PDF files. It can be seen from Fig. 1(1) that the calibration graph $a(x)$ can be considered linear in the whole range of x from 0 to 1. It is also seen that the tetragonal structure undergoes a phase transition into a cubic phase in the region of $x = 0.6$. Thorough investigations [2,3,16] showed that the $a(x)$ is not strictly linear near the phase transition when approaching the cubic phase but the deviation is minimal.

The same PDF files as above were used to plot a $\rho(x)$ calibration graph (Fig. 1(2) for calculating the theoretical values of density ρ_{th}. If prepared ceramics had two phases then $\rho_{th} = \rho_{th}(x_1) \times S_1 + \rho_{th}(x_2) \times S_2$, where S_1 and S_2 are the shares of the phases 1 and 2 (see Table 1). The ρ_{th} values are needed to compare densities of different samples. The apparent (measured) densities ρ_{app} cannot be compared directly, as they do not take into account the differences of phase contents and need to be related to the theoretical densities $\rho\ (\%) = (\rho_{app}/\rho_{th}) \times 100$. The apparent density was measured in water using the Archimedes principle as follows:

$$\rho_{app} = \frac{M_a}{M_a - M_w} \times \rho_w \quad (1)$$

where M_a is mass of sample in air, M_w is mass in water, and ρ_w is the density of water.

Microstructure and the grain content analyses were performed using a Philips XL-30S Scanning Electron Microscope combined with an Energy Dispersive Spectrometer (EDS).

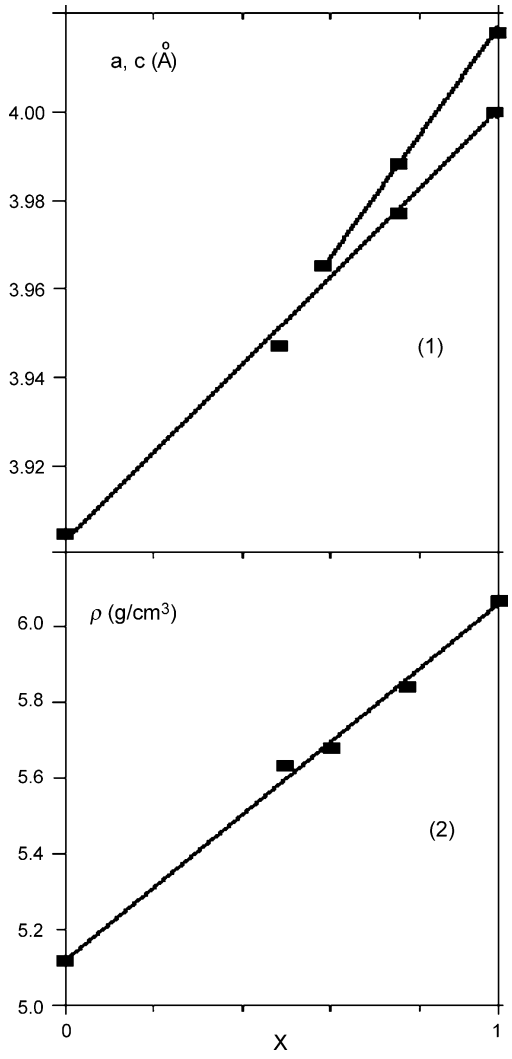

Fig. 1. Calibration graphs $x(a, c)$ and $x(\rho)$, where a and c are lattice parameters and ρ is density of BST compounds. The parameters are obtained from 79-2265, 34-0411, 44-0093, 39-1395 and 79-0175 PDF library numbers (see [2,3,16]).

Dielectric properties were measured using a HP 4294A Precision Impedance Analyzer, either in a silicon oil bath (0–120 °C) or in liquid nitrogen (liqN_2 to 20 °C) at 1 kHz frequency. The samples were sliced and thinned down to 0.50 mm thick discs. Silver paste was applied on both sides of the discs for electrical contacts. The dielectric constant was calculated from the capacitance using the following formula:

$$\varepsilon = \frac{C \times d}{\varepsilon_0 \times A} \quad (2)$$

where C is the capacitance, ε_0 the free space dielectric constant (8.85×10^{-12} F/m), A and d are the surface area and the thickness of the samples.

4. Experimental results

4.1. Phase content

It is known that sintering of BST powders into solid specimens provides further beneficial conditions on phase

Table 1
Ba is a share of barium in the initial mixture (Ba/Ba + Sr), t is a sintering time at 1300 °C in hours, a_1 and a_2 are the cell parameters of the phases in angstroms, x_1 and x_2 are the parameter x in $Ba_xSr_{1-x}TiO_3$ phases derived from the position of the calculated (1 1 1) peaks after the peak fit program was used (Fig. 2) and the Vegard's law was applied (Fig. 1(1)).

Ba	t (h)	a_1 (Å)	a_2 (Å)	x_1	x_2	w_1 (nm)	w_2 (nm)	S_1/S_2	T_{c1} (°C)	T_{c2} (°C)	ρ_{app} (g/cm^3)	ρ (%)
0.9	1	3.9795		0.79		21			37		5.59	95
0.9	3	3.97649		0.78		22			45		5.63	96
0.9	5	3.97793		0.77		23			52		5.35	91
0.9	8	3.9806		0.79		22			53		5.2	88
0.85	1	3.97503	3.9545	0.74	0.53	20	23	81/19	20		5.61	97
0.85	3	3.97285	3.95368	0.72	0.52	24	27	86/14	14	−44	5.73	99
0.85	5	3.97122	3.9609	0.70	0.60	20	25	72/28	19	−40	5.57	97
0.85	8	3.97338	3.96018	0.72	0.59	20	23	70/30	23		5.41	96
0.8	1	3.9617	3.94032	0.6	0.38	27	33	78/22	−4	−72	5.43	96
0.8	5	3.96087	3.9434	0.59	0.41	30	30	78/22	−5	−66	5.25	93
0.8	8	3.95756	3.93867	0.56	0.36	28	41	86/14	−19	−69	5.21	93
0.75	1	3.9473	3.93764	0.45	0.35	23	30	46/54	−66	−104	5.23	95
0.75	3	3.9471	3.93773	0.45	0.35	41	46	23/77	−66	−100	5.23	96
0.75	5	3.94669	3.93916	0.45	0.37	22	31	37/63	−68	−97	5.3	96
0.75	8	3.94302	3.93787	0.41	0.35	30	43	31/69	−69	−104	5.34	96

w_1 and w_2 are the crystal sizes calculated from the peak width using Schrerrer's formula (3). S_1/S_2 are ratios of the areas under the calculated peaks. This value shows the relative amounts of the phases in the BST. T_{c1} and T_{c2} are the Curie temperatures of the phases in degrees of Celsius obtained from the $\varepsilon(T)$ dependencies (Fig. 4), ρ_{app} is apparent density calculated from formula (1), and ρ is apparent density relative to the theoretical density of the samples in percent.

transformation and homogeneity of samples because of high temperature inter-diffusion of barium and strontium ions between the grains [17,18]. During sintering grain growth takes place, crystallinity improves and, as a result, density increases [18,19].

XRD spectra of the sintered samples showed no other peaks of secondary phases than those of the BST compounds. Almost all of the spectra exhibited asymmetrical peaks (Fig. 2) indicating, as in the previous work [11], that the ceramics was still a mixture of more than one $Ba_xSr_{1-x}TiO_3$ phase, even after sintering. To separate contributions of different phases into the experimental spectra a peak fit program was used. Because of too many unknown parameters the fit was performed on one peak first, assuming that it was a double peak. This assumption is based on our previous calculations [11] where it was found that the raw ceramic powder consisted of two BST phases. It is safe to assume that the number of phases does not increase after sintering. Then, the parameters obtained from the peak fit were tried to fit the whole spectrum. If the result was negative the peak fit was run again with slightly different initial parameters until the results satisfied the whole spectrum. This method is semi-quantitative, and it can only be applied for evaluation purposes. The described procedure is different from the Rietveld method where all the information about the compounds in the mixture needs to be known before the calculation start. To perform fit (1 1 1) peak was chosen as it remains a single peak in the whole range of $Ba_xSr_{1-x}TiO_3$ from Ba-rich tetragonal ($1 < x < 0.6$) to Sr-rich cubic ($0.6 < x < 0$) phase. For comparison, other strong peaks such as (1 1 0) may split into (1 1 0) + (1 0 1) or become (1 0 1) one, (2 0 0) peak splits into (2 0 0) + (0 0 2)

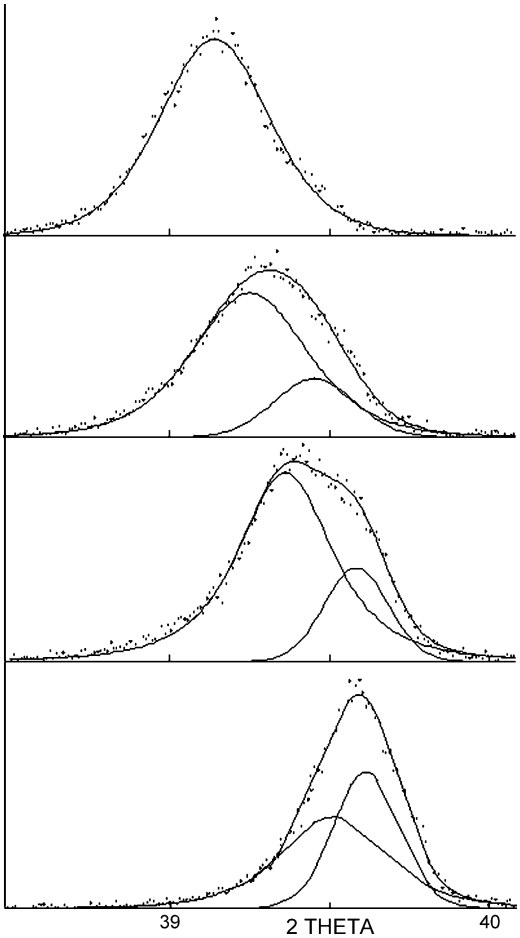

Fig. 2. Experimental (1 1 1) peaks of Ba/(Ba + Sr) = 0.9, 0.85, 0.8, 0.75 (from top to bottom) and the results of the peak fit calculations.

in the tetragonal phase. Fig. 2 shows the calculated peaks of the samples after the first hour of sintering. From the position of the calculated peaks their a and c cell parameters were derived. Substituting these values into the $x(a)$ graph (Fig. 1(1)) the x parameter of the both phases (x_1 and x_2, Table 1) in the powder were obtained. The relative areas of the calculated peaks S_1 and S_2 were assumed to be proportional to the amounts of the phases in the powder. The results of the calculations are listed in Table 1.

Similar calculations were applied to the raw, as reacted, non-sintered BST powder in our previous work [11]. Fig. 3 compares the samples contents before and after the sintering. It is seen that interdiffusion of Ba^{2+} and Sr^{2+} occurs in both Ba- and Sr-rich phases during the sintering process as the peaks move towards each other. The sample with the smallest initial value of Sr (Ba/(Ba + Sr) = 0.9) becomes single phased. All of the other samples, though their homogeneity is improved, remained double phased, even after sintering time was increased up to 8 h.

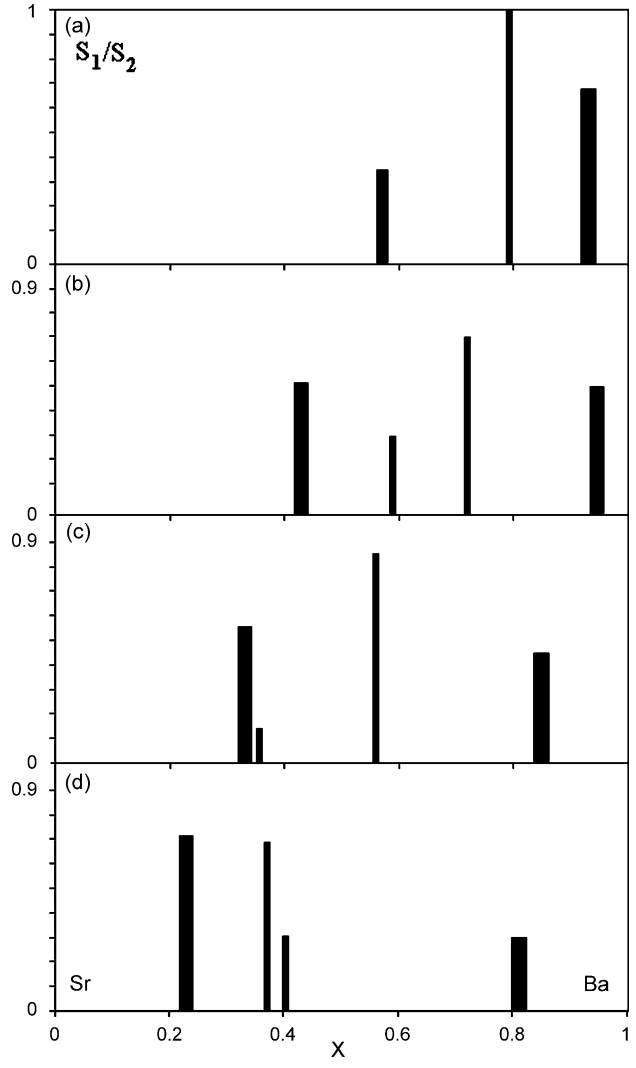

Fig. 3. Phase content of the samples before (reported earlier [11]) and after sintering. The solid lines represent position (parameter x) and volume (height) of the phases before sintering and thin lines—after sintering. (a) Ba/(Ba + Sr) = 0.9, (b) 0.85, (c) 0.8 and (d) 0.75.

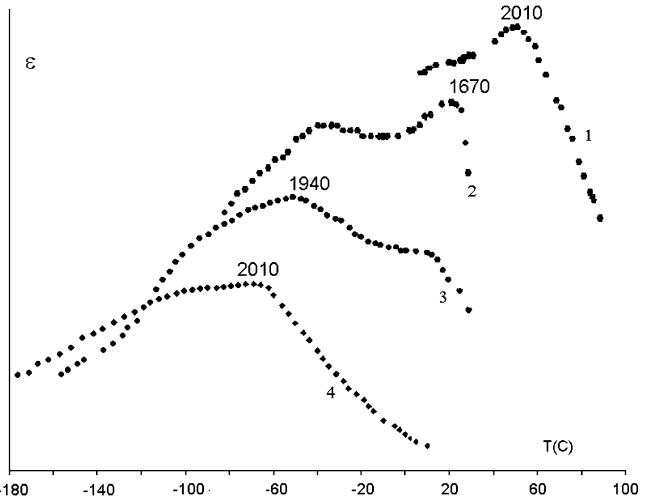

Fig. 4. $\varepsilon(T)$ dependencies of the samples prepared with the initial Ba/(Ba + Sr) ratio of 1–0.9, 2–0.85, 3–0.8, 4–0.75 and sintered for 5 h at 1300 °C. Figures show the ε values at the maximum of the plots. The plots are shifted vertically for a better view.

4.2. Electrical properties

Temperature behavior of dielectric constant ε of the samples sintered for 5 h is shown in Fig. 4. It is seen that the samples have either single peak or double peak $\varepsilon(T)$ dependencies, reflecting their complex phase contents. The peak temperatures T_c are listed in Table 1 and plotted in Fig. 5 against the barium content x. It is seen that the experimental points follow a linear

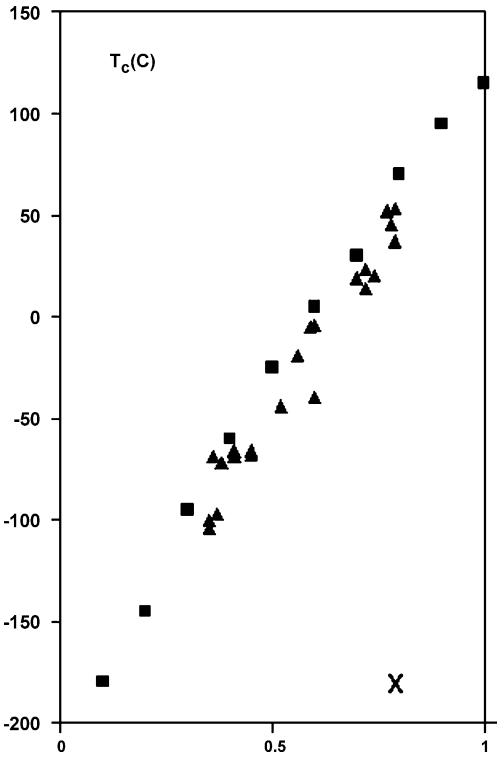

Fig. 5. Curie temperature T_c (triangles) versus the structural parameter x of all of the studied samples. Squares show the values obtained by the conventional solid state technique [16,20].

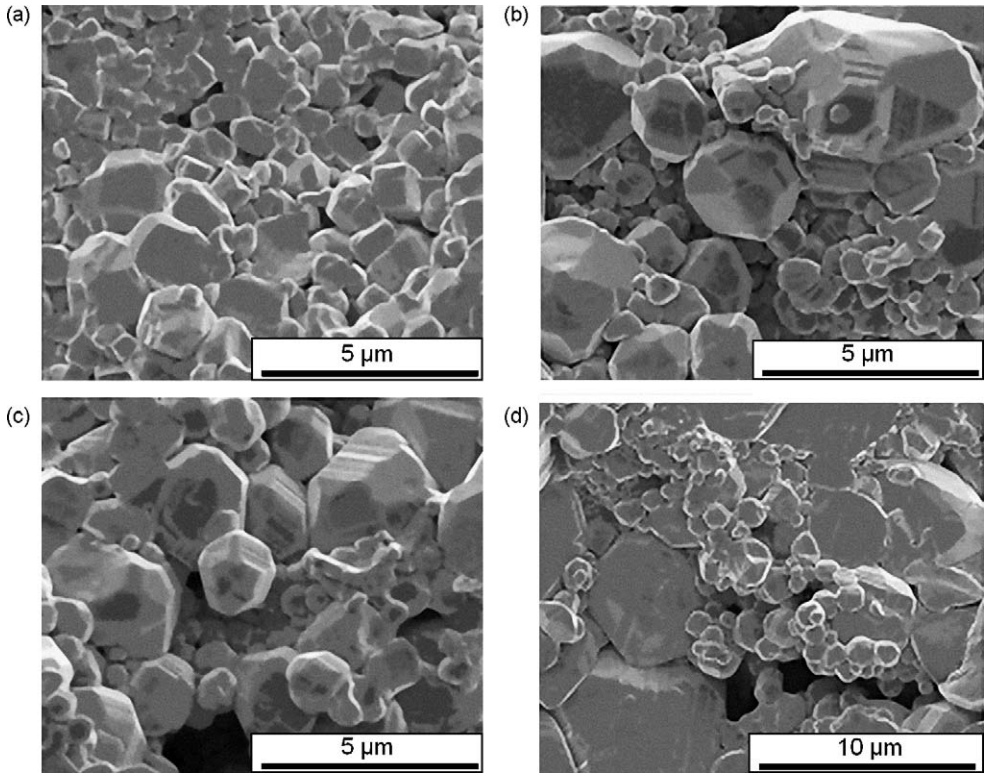

Fig. 6. Microstructure of samples prepared with the initial ratio of Ba/(Ba + Sr) (a) 0.75, (b) 0.8, (c) 0.85, (d) 0.9 and sintered at 1300 °C for 1 h.

dependence $T_c(x)$ typical for data obtained from a conventional solid state technique and superimpose them [1,16,20]. The absolute values of ε, though, are almost one order smaller, and the dependencies near the Curie transition point are broadened. It is quite possible that the ferroelectric properties of the samples are suppressed because of the small nanosize of the crystals in the range of 20–50 nm (Table 1) [21,22].

4.3. Structural parameters

Fig. 6 shows how the microstructure changes for a small sintering time of 1 h when the initial Ba/(Ba + Sr) ratio was decreased from 0.9 to 0.75. It is seen that the samples, typically for BST compounds, have a mixture of big Ba-rich grains and a matrix of small Sr-rich grains [11,14], confirmed by our EDS analysis. The ratio between them changes with the Ba/(Ba + Sr) value. It is seen from Fig. 7a that the best grain packing arrangement occurred when the initial barium share was 85%.

Surprisingly, as Table 1 shows, none of the structural and phase parameters of the samples undertook any significant changes when the sintering time was increased from 1 to 8 h. SEM pictures (Fig. 8) show a rapid growth of the grain size, however, the sample densities (Fig. 7b), phase content x, the relative amount of the phases S_1/S_2, estimated from the areas under the peaks, and the crystal size w, though larger compared to the original, non-sintered powder (11–20 nm) [11], remained almost unchanged. The exception was the 90% Ba sample (Fig. 7b) which density dropped 8% after sintering time

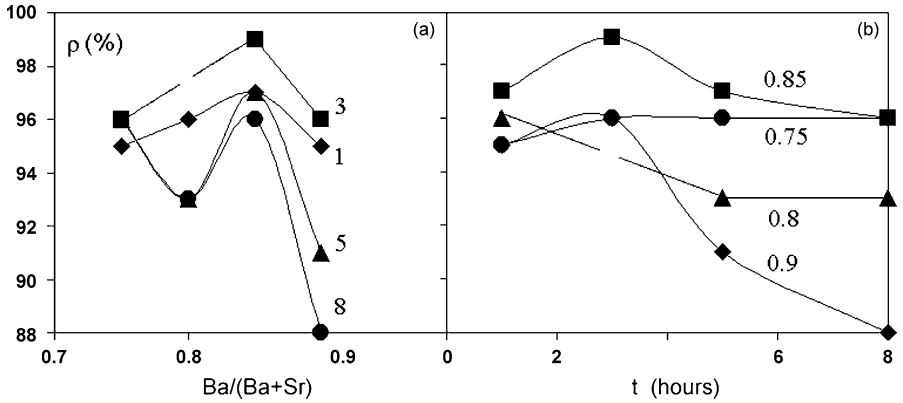

Fig. 7. Dependence of density of samples (ρ (%) = (ρ_{app}/ρ_{th}) × 100) from (a) the initial Ba/(Ba + Sr) ratio, numbers 1, 3, 5, 8 indicate sintering time in hours. (b) The same data plotted against the sintered time, numbers show the Ba/(Ba + Sr) values.

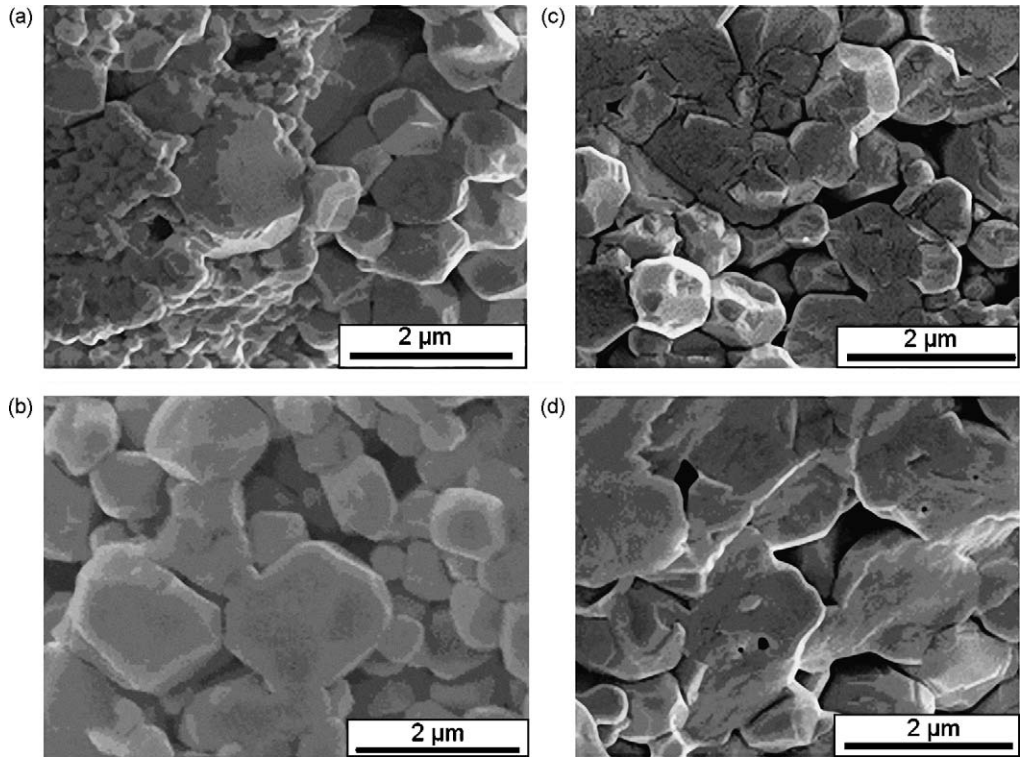

Fig. 8. Microstructure of samples prepared with the initial ratio of Ba/(Ba + Sr) = 0.9 and sintered at 1300 °C for (a) 1 h, (b) 3 h, (c) 5 h and (d) 8 h.

increased from 3 to 8 h. w was calculated from the Full Width at Half Maximum (FWHM) of the peaks, using the Schrerrer's relation:

$$w = \frac{0.9 \times \lambda}{(B_m^2 - B_s^2)^{1/2} \cos\theta}, \quad (3)$$

where λ is the X-ray wavelength, B_m and B_s are the experimental and instrumental FWHMs values, respectively.

5. Conclusion

The phase content of the BST ceramics prepared by the high temperature hydrothermal reaction and then sintered at 1300 °C for 1–8 h was successfully computed from the XRD spectra. The electrical properties of the samples were in good agreement with the results of the calculations.

It was shown that the ceramics with the initial molar ratio of Ba/(Ba + Sr) = 0.9 had a uniform phase content and a Curie temperature at 37–53 °C (Table 1). When the initial share of barium was reduced by 5% down to Ba/(Ba + Sr) = 0.85 the Curie point decreased down to room temperature (14–23 °C) but the phase analysis showed the presence of the second BST phase with the Curie point at −40 to −44 °C. Further reduction of barium still produced a double phased BST ceramics with Curie temperatures following a liner dependence of $T_c(x)$ in the whole range $0 < x < 1$ (Fig. 5). The absolute values of the dielectric constant were much smaller compared to the solid state technique samples and the $\varepsilon(T)$ ferro-paraelectric peaks were much broader. These are explained by the nanosize of ceramic crystals produced by the hydrothermal technique.

The crystal size of the ceramics doubled in size compared to the raw powder after the first hour of sintering, but when the sintering time was increased from 1 to 8 h, it did not change significantly and remained in the nanoscale.

Acknowledgement

Authors would like to thank Dr. J. Yoo for his help with the dielectric properties measurements.

References

[1] E.N. Bunting, G.R. Shelton, A.S. Creamer, Properties of barium–strontium titanate dielectrics, J. Am. Ceram. Soc. 30 (4) (1947) 114–125.
[2] D.F. Rushman, M.A. Strivens, The permittivity of polycrystals of the perovskite type, Trans. Faraday Soc. 42A (1946) 231–238.
[3] R.H. Dungan, D.F. Kane, L.R. Bickford, Lattice constants and dielectric properties of barium titanate–barium stannate–strontium titanate bodies, J. Am. Ceram. Soc. 35 (12) (1952) 318–321.
[4] D.E. Kotecki, J.D. Baniecki, H. Shen, R.B. Laibowitz, (Ba,Sr)TiO_3 dielectrics for future stacked-capacitor DRAM, J. Res. Dev. 43 (11) (1999) 367–382.
[5] Y.C. Choi, B.S. Lee, Bottom electrode dependence of the properties of (Ba,Sr)TiO_3 thin film capacitors, Mater. Chem. Phys. 61 (2) (1999) 124–129.
[6] X. Liang, W. Wu, Z. Meng, Dielectric and tunable characteristics of barium strontium titanate modified with Al_2O_3 addition, Mater. Sci. Eng. B 99 (1–3) (2003) 366–369.
[7] B. Su, T.W. Button, The processing and properties of barium strontium titanate thick film for use in frequency agile microwave circuit applications, J. Eur. Ceram. Soc. 21 (15) (2001) 2641–2645.
[8] B. Su, J.E. Holmes, C. Meggs, T.W. Button, Dielectric and microwave properties of barium strontium titanate (BST) thick films on alumina substrates, J. Eur. Ceram. Soc. 23 (14) (2003) 2699–2703.

[9] J. Xu, W. Menesklou, I.-T. Ellen, Processing and properties of BST thin films for tunable microwave devices, J. Eur. Ceram. Soc. 24 (6) (2004) 1735–1739.
[10] H. Abdelkefi, H. Khemakhem, G. Velu, J.C. Carru, R. Von der Muhll, Dielectric properties and ferroelectric phase transitions in $Ba_xSr_{1-x}TiO_3$ solid solution, J. Alloy Compd. 399 (1–2) (2005) 1–6.
[11] K.A. Razak, A. Asadov, W. Gao, Properties of BST ceramics prepared by high temperature hydrothermal process, Ceram. Int. 33 (8) (2007) 1495–1502.
[12] K.A. Razak, A. Asadov, J. Yoo, W. Gao, E. Haemmerle, Structural and dielectric properties of barium strontium titanate produced by high temperature hydrothermal method, J. Alloy Compd. 449 (2008) 19–23.
[13] K.A. Razak, A. Asadov, J. Yoo, M. Hodgson, E. Haemmerle, Characterization of BST produced by high temperature hydrothermal synthesis, Int. J. Mod. Phys. B 20 (25–27) (2005) 4153–4158.
[14] R.K. Roeder, E.B. Slamovich, Stoichiometry control and phase selection in hydrothermally derived $Ba_xSr_{1-x}TiO_3$, J. Am. Ceram. Soc. 82 (7) (1999) 1665–1675.
[15] K. Kajiyoshi, K. Tomono, Y. Hamaji, T. Kasanami, Short-circuit diffusion of Ba, Sr, and O during $ATiO_3$ (A = Ba, Sr) thin film growth by the hydrothermal—electrochemical method, J. Am. Ceram. Soc. 78 (6) (1995) 1521–1531.
[16] Landolt-Bornstein. Numerical data and functional relationships in science and technology. New Series, Group III: Crystal and Solid State Physics, vol. 16, Ferroelectrics and related substances, Subvolume a: Oxides, 1981, p. 416.
[17] D. Kollar, M. Trontelj, Z. Stadler, Influence of interdiffusion on solid solution formation and sintering in the system $BaTiO_3$–$SrTiO_3$, J. Am. Ceram. Soc. 65 (10) (1982) 470–474.
[18] S. Nomura, Solid state reaction between barium titanate and strontium titanate, J. Phys. Soc. Jpn. 11 (9) (1956) 924–929.
[19] M.N. Rahaman, Ceramic Processing and Sintering, 2nd ed., Marcel Dekker, Inc., New York, 2003.
[20] C. Fu, C. Yang, H. Chen, Y. Wang, L. Hu, Microstructure and dielectric properties of $Ba_xSr_{1-x}TiO_3$, Mater. Sci. Eng. B 119 (2005) 185–188.
[21] L. Zhang, W.-L. Zhong, C.-L. Wang, P.-L. Zhang, Y.-G. Wang, Finite-size effects in ferroelectric solid solution $Ba_xSr_{1-x}TiO_3$, J. Phys. D: Appl. Phys. 32 (1999) 546–551.
[22] K. Kinoshita, A. Yamaji, Grain size effect on dielectric properties in barium titanate ceramics, J. Appl. Phys. 47 (1) (1976) 371–373.